ISSN 1392-1207. MECHANIKA. Vol. 31, No. 3, 2025: 199–210

Synthesis and Rheological Characterization of Magnetorheological Fluids

Vinod CHAUHAN, Ashwani KUMAR, Radhey SHAM
Department of Mechanical Engineering, Chandigarh College of Engineering & Technology (Degree Wing), Chandigarh, India, 160019, E-mails: vinodchauhan@ccet.ac.in, ashwanikumar@ccet.ac.in, radheysham@ccet.ac.in
https://doi.org/10.5755/j02.mech.37200

1. Introduction

Smart materials can vary their rheological characteristics while subjected to some external magnetic field. The MR fluid also corresponds to this class of materials. These fluids alter their yield strength with variation of the magnetic field. The iron (Fe) particles orient along the magnetic flux lines (Fig. 1) when exposed to the magnetic field. This helps in the formation of strong particle chains, which results in higher yield stress values. The chain-like arrangement constrains the fluid flow, consequently enhancing the viscous attributes of the prepared suspensions. The yield stress indicates the stress needed to rupture the chain-like pattern of the Fe particles [1]. Premalatha et al. [2] prepared MR fluids and analyzed their flow behavior in terms of stability, internal structure, and MR characteristics. Silicone oil, iron powder, and grease have been used for synthesizing the MR fluid. The particle size and flow characteristics have been observed by employing an optical microscope and a rheometer respectively. The shear thinning behavior has been observed, and storage modulus along with loss modulus values are enhanced, indicating stronger elastic interactions. Mangal and Kumar [3] synthesized various MR fluids with variations in weight proportions of Fe particles suspended in silicon oil. The results exhibit that the MR fluid yield stress values improved by the intensification of Fe particles.

Kamble et al. [4] developed MR fluids by selecting Fe particles as dispersed phase & castor oil, and honge oil as carrier medium. The fluid containing honge oil exhibits greater viscosity as compared to that containing castor oil. Shear stress has been enhanced with the shear rate, which depicts that prepared fluids follow the Bingham plastic model. Sarkar et al. [5] analyzed the demagnetization effect by including the nano-copper and nano-silver particles in MR fluids. The inclusion of these particles ensures the reduction in heat generation during the operation of the MR brake. Liu et al. [6] synthesized heat transfer oil-based MR fluid utilizing oleic acid reworked CI particles as a dispersal phase and strontium hexaferrite nano-sized particles as additives. The results exhibit a remarkable improvement in the sedimentation stability of the prepared MR fluid. The impact of added nanoparticles, magnetic field strength, and temperature has been investigated. Jain and Avchare [7] synthesized various MR fluid samples for brakes containing micron-sized iron particles, silicone oil, and tetra-methylammonium oxide. The generated torque mostly relies on the concentration of Fe particles suspended in the MR Fluid. Vėžys et al. [8] diagnosed the sedimentation of MR fluids by measuring their electric resistivity in the presence of a magnetic field. During this process, a specially designed device was used to estimate the electrical resistivity. Arief et al. [9] investigated the MR characteristics of MR fluids containing CoNi microclusters. The Co-rich microclusters have been prepared using conventional homogeneous nucleation in liquid polyol. The room temperature magnetization and crystal structure measurements have been obtained by vibrating sample magnetometry. The results indicate a decline in the MR characteristics at elevated temperatures. Guo et al. [10] introduced a preparation process for MR fluids containing varying grain diameters (3 μm & 10 μm) of CI particles. The MR fluid, having CI particles of 10 μm size, showed higher zero field viscosity and on state yield stress (OYS) but degraded sedimentation stability. Laherisheth and Upadhyay [11] investigated the impact of adding the nanoparticles in spherical-shaped and irregular flake particle-based MR fluids. The dispersal of nanoparticles mitigates the friction between the particles because the nanoparticles get attached to the surface magnetically and act as a nano-lubricant. The value of saturation magnetization is enhanced by 15 percent for the flake-based MR fluid but remains almost unchanged for spherical particle-based MR fluids. Gurubasavaraju et al. [12] identified the impact of MR fluid constituents, current, & the fluid gap on the rheological attributes and damping of the MR damper using particle swarm optimization. Three different MR fluids with 25%, 30%, and 35% volume proportions of CI particles included in a silicone carrier medium and 1% of lithium grease have been prepared. The interactions for the regression model achieved by the design of experiment technique have been used in particle swarm optimization to estimate the optimal parameters.

Lijesh et al. [13] prepared the MR fluid that is highly dispersible, has lower off-state viscosity, and has higher values for on-state shear stress. A stable suspension of CI particles using oleic acid and tetramethyl ammonium hydroxide has been obtained. The MR fluid having 0.25 percent oleic acid exhibits a lower value of off-state viscosity & shear stress and a greater value of on-state viscosity & shear stress. In addition to this, increasing the proportion of tetramethyl ammonium hydroxide in MR fluid enhances on-state shear stress and improves sedimentation stability. Nagdeve et al. [14] synthesized the MR finishing fluids by using abrasive particles (boron carbide) of varying sizes (4, 6, and 9 microns) along with CI particles having a particle size of 6 microns. The prepared fluid samples contain 25% CI particles and 10% abrasive particles suspended in a paraffin oil carrier medium. The results indicate that the MR fluid containing the same size of CI and abrasive particles indicates greater yield stress values relative to other mixtures. The size, hardness, and concentration of elements of MR fluid remarkably impact the performance of the

finishing process. Guo et al. [15] coated the CI particles with the multi-wall carbon nanotubes using the ultrasonication technique and used a mechanical stirrer setup to synthesize the MR fluid. The coating impact on CI particles has been investigated through surface topography, particle density, and stability testing of the synthesized MR fluids. The outcomes show a negligible decline in the magnetic saturation, but the adsorption force between particles, along with particle density reduced significantly, thereby bettering the sedimentation stability. Dorosti et al. [16] made use of worm-like micelles (WLMs) to improve the rheological attributes of water-based MR fluids. Cetyltrimethylammonium ammonium bromide has been used as a dispersal medium along with potassium bromide. The WLMs structure has been investigated using a cryo-scanning electron microscope and static light scattering technique. The inclusion of WLMs improves the sedimentation rate and yield stress of the prepared MR suspensions.

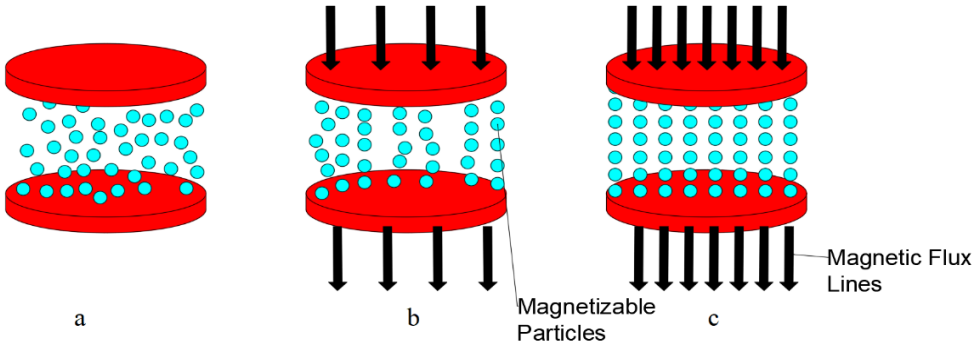

Fig. 1 Schematic diagram of MR fluid a – in absence of a magnetic field, b – in presence of a weak magnetic field, c – in presence of a strong magnetic field

Vėžys et al. [17] compared two methods, i.e., electrical resistivity and inductivity measuring methods, to describe the long-term sedimentation stability in various MR fluids. The correlation coefficients were determined to estimate the strength of the relationship between the relative movements of the variables. Marins et al. [18] focus on the MR characterization of fluids containing Fe particles and sepiolite fiber (thickening agent). The composite MR fluid exhibits a progressive rise in the field-induced static yield stress with a rise in the volume proportion of Fe particles. The addition of sepiolite fibers gives rise to perfect sedimentation stability, moderate plastic viscosity, moderate off-state static yield stress, and comparatively significant improvement in static and dynamic yield stress. Zhu et al. [19] utilized the DC arc discharge method to synthesize the iron nanoparticles. The magnetic properties, crystal structures, and morphology of the prepared nanoparticles have been investigated. The micron and nano-sized CI particles are suspended in a carrier fluid to prepare the MR fluid. The inclusion of Fe nanoparticles into MR fluid exhibits a significantly improved sedimentation stability but slightly lowers the MR effect. Aruna et al. [20] focus on mitigating the sedimentation ratio of the MR fluids. The CI particles are diffused in a poly alpha-olefin oil, and the inclusion of additives (Clayton APA, baragell 10, etc.) along with a friction reducer agent (molyvan 855) significantly improves the sedimentation rate. Jinaga et al. [21] utilized carrier fluid (a blend of organic oil, silicon oil, honey, cottonseed oil, and sunflower oil), coated EI particles, and oleic acid. The blended MR fluid exhibits a 10 percent betterment in sedimentation stability in comparison with the conventional type of MR fluid. The fluid containing cottonseed oil presents better sedimentation stability in comparison with the sunflower-based fluid. Zhang et al. [22] prepared MR fluid samples with varying magnetic particle concentrations (10%, 28%, and 28%) suspended in silicon oil. The shear stress obtained experimentally at various magnetic field densities has been analyzed using the Herschel-Bulkley model, Seo-Seo model, and a new modified model. The results exhibit that the newly developed model (modified model) fits well as compared to other used models. Seo and Choi [23] highlighted the latest advances in the synthesis of Fe_3O_4 nanocomposites with a core-shell structure and their merits & MR characteristics. Unlike metallic Fe particles, the soft-ferrimagnetic Fe_3O_4 spherical particles used in MR suspensions are quite reliable & efficient, and exhibit higher suspension stability in the long-term use. Huang et al. [24] developed a novel structure for the MRF damper to monitor & improve the MR fluid's long-term sedimentation stability. The structural variables/parameters of the MRF damper were obtained using numerical analysis. The sedimentation stability of the novel structured MRF damper was enhanced by nearly 20% in comparison with the conventional MRF damper. Srivastava et al. [25] developed a double-disc chemically-assisted type MR finishing mechanism to polish brittle material, namely monocrystalline silicon wafer, and utilized a vibrating sample magnetometer for obtaining the saturation magnetization of the fluid. Herschel-Bulkley along with Casson's fluid model, better fit the rheological data in comparison to the Bingham-Plastic model. The shear-thinning has been noticed due to the breakdown of dense CI-particle chains at greater shear rates. Viscosity and shear stress are reduced with the rise in the fluid temperature.

Xu and Sun [26] proposed a single-double chains micro-mechanical MR fluid model considering the impact of magnetic induction and volume proportion on the microstructure. The MR fluid containing multiwall carbon nanotubes along with graphene oxide-coated magnetic particles has been prepared, and the results indicate a better fitting of the single-chain model when the particle proportion is lower than 25%. When particle proportion is greater than 25%, the single-chain model fits better at lower magnetic strength, and the double-chain model is better fitted at higher magnetic strength. Maurya and Sarkar [27] prepared water-based MR fluids containing micron-sized flake-shaped CI particles, oleic acid as a surfactant, and laponite as an additive. The addition of oleic acid and laponite significantly

bettered the sedimentation rate for the prepared MR suspension. The MR fluid with a higher laponite proportion is more effective at a low magnetic field, but the MR fluid containing a smaller laponite proportion becomes more effective at a greater magnetic field. The laponite-based suspensions exhibit excellent resistance to particle aggregation and settling issues. Han et al. [28] investigated the magnetic particle's shape effect on MR performance and stability of prepared MR suspensions. A flaky sendust powder exhibited higher yield stress even at lower magnetic fields due to the shape anisotropy effect that causes a rapid rise in the magnetic moment of the particles. Despite having a lower Fe content (85%) as compared to CI (99%), the sendust powder suspension produced a higher yield stress at lower magnetic field strengths. The flaky sendust suspensions exhibit higher sedimentation stability compared to bulk sendust suspensions and CI suspensions because of their larger drag coefficient.

Gedik et al. [29] investigated three types of MR fluids flowing in circular pipes of varying diameters (10 mm and 15 mm) under zero-field and magnetic field conditions. The magnetic field rise enhances the MR fluid's viscosity and reduces the flow velocity (flow velocity dropped by 95% at B = 0.15 Tesla). The results obtained experimentally and using an artificial neural network algorithm model follow each other. Choi [30] discussed various techniques to better the sedimentation rate of MR fluids. The particle modification stage includes particle shape, weight concentration, coating of materials, size distribution, and combinations of various particle sizes, while carrier medium modification includes wettability control, density increment, wettability, and the use of natural oils, grease, ethyl-butylacetate oils, lubricant oil, grease, etc. Tong et al. [31] used a mixture of silicone oil and ionic liquid as the carrier medium to prepare the MR fluid. The prepared fluid has been compared with the fluid containing pure silicone oil and pure ionic liquid as carrier medium. The results illustrated that the MR fluid, having a mixture of silicone oil & ionic liquid, exhibits a better sedimentation rate and greater yield stress than the other two prepared fluids. Kumar et al. [32] prepared MR fluid containing CI particles, graphene oxide, and iron oxide nanocomposite particles. A blended oil containing 90% rice bran oil and 10% silicone oil has been used carrier medium to ensure economic and environmental feasibility. The magnetic saturation improves due to the encapsulation of graphene oxide-decorated iron oxide nanocomposite particles. The coefficient of friction and wear were reduced remarkably, resulting in a lubricating protective layer at the contact interface. Zhao et al. [33] examined the microstructure & shear attributes of the interface between dimethyl silicone oil and CI particles using molecular dynamics simulation. The adhesive strength was enhanced considerably between dimethyl silicone oil and Fe atoms on the CI particle's surface during the shearing phenomenon. The MR fluids using low viscosity dimethyl silicone oil (50-200 mPa-s) indicated a weaker molecular structure (easy to break), while the use of higher viscosity dimethyl silicone oil (350-500 mPa-s) ensured a stronger molecular structure and high interfacial shear strength. Maharani et al. [34] discussed that the actuating properties of MR fluids declined significantly after the sedimentation, which was related to the long-term effects of temperature and magnetic fields. This is most likely caused by the degradation of the rheological properties (viscosity, shear stress, yield stress) of MR fluids. Horak et al. [35] studied shear stress variations of MR fluids subjected to comparatively large deformations during successive loading cycles as well as the shifts during the rest phase. The study investigated the real-time variations in shear stress associated with discontinuous deformations, i.e., pauses in deformation. Wiener et al. [36] developed a model for determining the dynamically varying Fe content during operation of the MR actuator, which predicted the real-time actuator behavior with greater precision. The inductance of the used magnetic circuit was used to estimate the Fe concentration in the MR working gap. The developed model monitored the Fe content, eliminating the need for any offline analysis.

2. Synthesis of MR Fluids

The selection of appropriate carrier fluid, micron-sized magnetic particles, and suitable additives has a pivotal role in synthesizing MR fluids. The in-house mechanical stirrer setup utilized to synthesize the MR samples is shown in Fig. 2.

2.1. Constituents of MR fluid

The MR fluid contains a carrier medium, magnetic micron-sized magnetic particles, and surfactants/additives. In the present study, the chosen constituents for synthesizing the MR fluid are carrier fluid (Castor oil and silicon oil), Iron particles namely carbonyl iron of 6-micron size (CI6), electrolytic iron of 16-micron size (EI16), and electrolytic iron of 32-micron size (EI32), additive i.e. EGMS (Ethylene Glycol Monostearate) for enhancing the fluid's sedimentation stability.

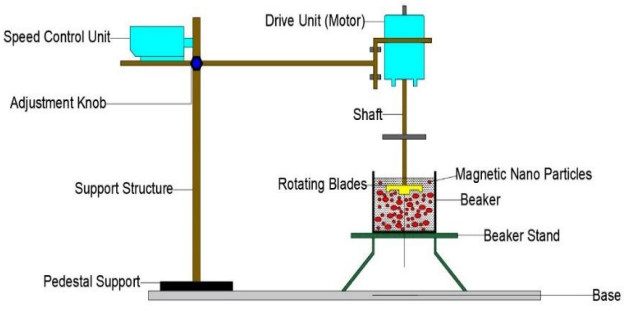

Fig. 2 Schematic illustration of the Mechanical Stirrer

2.2. Morphology of the magnetic particles

The CI and EI iron (Fe) particles of varying sizes are utilized for preparing the MR fluids. The detailed structure of three types of Fe particles and their size distribution, performed using FESEM (Field emission scanning electron microscopy), has been presented in Fig. 3, a, b, and c. The flake structure particles having an APS (average particle size) of 6 μm are presented in Fig. 3, a. The flake-shaped particles assist in superficial interactions with the used additive, making it a better dispersant. Fig. 3, b presents spherical and irregularly shaped Fe particles with an APS of 16 μm. Fig. 3, c exhibited sharp and irregularly shaped particles having an APS of 32 μm.

Energy Dispersive X-ray (EDS) testing results for CI6 Fe Particles, EI16 Fe Particles, and EI32 Fe Particles are shown in Fig. 4, a, b, and c, respectively. established that the particles used in the study mainly contain Fe particles and a very small amount of other elements such as carbon,

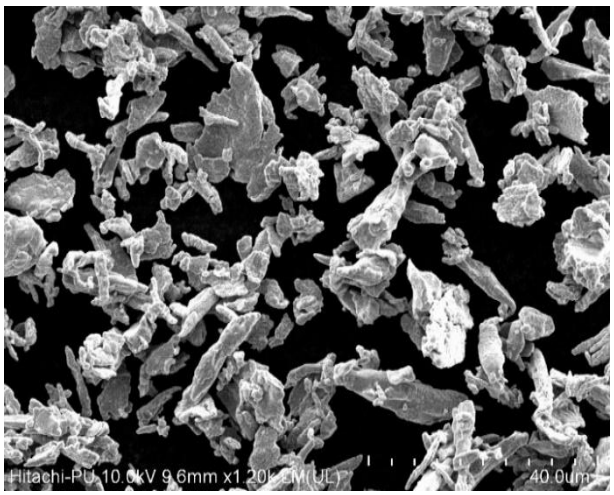

a

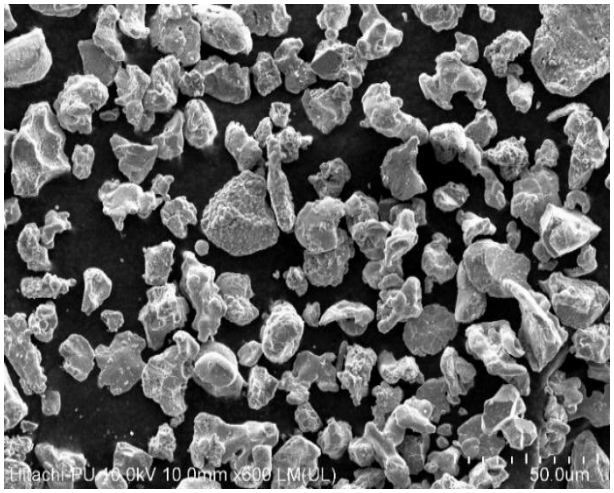

b

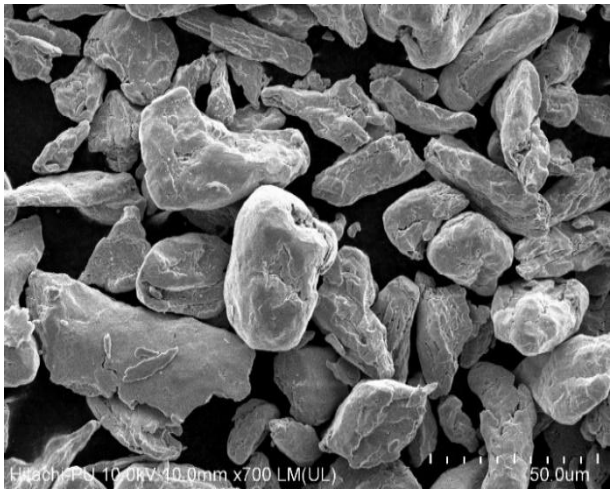

c

Fig. 3 FESEM images: a – CI6 Fe particles, b – EI16 Fe particles, c – EI32 Fe particles

oxygen, silicon, cobalt, nickel, copper, aluminum, etc.

2.3. Experimental design

Depending on the critical literature survey [37], four input parameters (Table 1) have been chosen for preparing the MR fluid. The carrier fluid parameter occupies two levels, while for the remaining parameters, namely iron

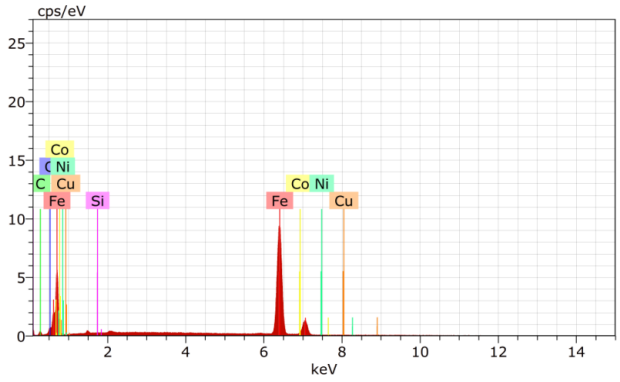

a

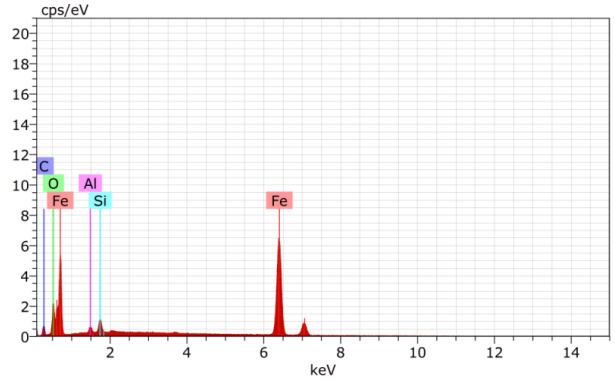

b

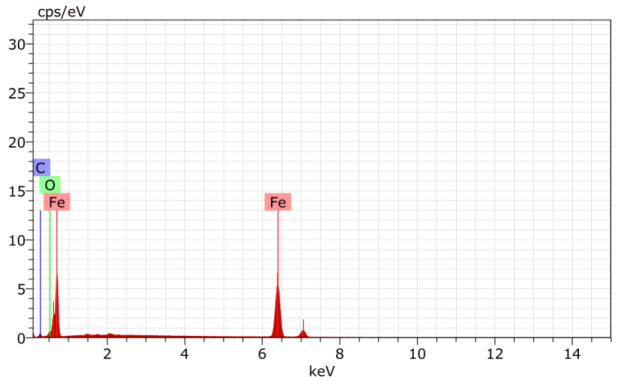

c

Fig. 4 EDS images: a – CI6 Fe particles, b – EI16 Fe particles, c – EI32 Fe particles

particle type, iron particle proportion (vol%), and EGMS (vol%), three levels have been taken. The 18 MR fluid samples have been synthesized using an in-house developed mechanical stirrer setup. Taguchi's L_{18} Orthogonal Array (OA) is utilized to obtain the most significant set of selected input parameters. The various assigned parameters using an L_{18} OA have been shown in Table 2.

Table 1

Input Parameters and their levels

S. No.	Parameters	Lower value	Mid Value	Upper Value
1	Carrier Fluid	Silicon oil	Castor oil	------
2	Iron Particle Type	CI6	EI16	EI32
3	Iron Particle Proportion (vol %)	16	20	24
4	EGMS (vol %)	1.0	1.5	2.0

Table 2

Selected Parameters Assigned to L_{18} OA

Sample No.	Carrier Fluid	Iron Particle Type	Iron Particle Proportion (vol%)	EGMS (vol%)
1	Silicon oil	CI6	16	1.0
2	Silicon oil	CI6	20	1.5
3	Silicon oil	CI6	24	2.0
4	Silicon oil	EI16	16	1.0
5	Silicon oil	EI16	20	1.5
6	Silicon oil	EI16	24	2.0
7	Silicon oil	EI32	16	1.5
8	Silicon oil	EI32	20	2.0
9	Silicon oil	EI32	24	1.0
10	Castor oil	CI6	16	2.0
11	Castor oil	CI6	20	1.0
12	Castor oil	CI6	24	1.5
13	Castor oil	EI16	16	1.5
14	Castor oil	EI16	20	2.0
15	Castor oil	EI16	24	1.0
16	Castor oil	EI32	16	2.0
17	Castor oil	EI32	20	1.0
18	Castor oil	EI32	24	1.5

3. Experimental Testing of MR Fluid

After the preparation of the MR fluid samples (Table 2), the sedimentation stability of the MR fluid samples has been investigated in-house, and an on-state testing of the fluid is done using an Anton Paar rheometer.

3.1. Sedimentation stability of MR fluid

The sedimentation behavior of the synthesized MR fluid samples has been analyzed. The sedimentation ratio is defined as the ratio of the volume of the transparent carrier fluid region above the settled particle layer to the total fluid volume prior to sedimentation, and is illustrated qualitatively for varying time interval in Fig. 5. The results indicate that increasing the proportion of the additive, EGMS, significantly improves the sedimentation stability of the synthesized MR samples. The data also indicates that the sedimentation ratio may be modulated to a certain extent by varying the proportion of used additives. Beyond a certain limit, the inclusion of additives adversely affects the MR

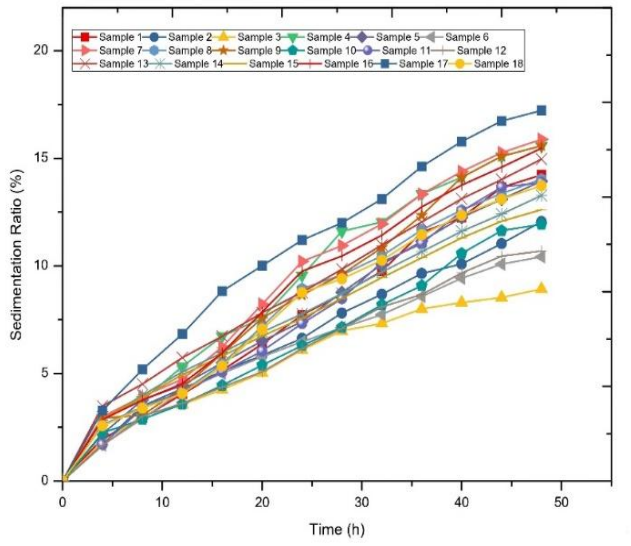

Fig. 5 Sedimentation results of 18 prepared MR fluid samples

3.2. On state testing of MR fluid

The experiments have been conducted on a rotational oscillatory shear rheometer, namely MCR-102 fluid's yield stress. Among the 18 synthesized MR fluid samples, Sample No. 3 stands out with the highest sedimentation stability. (modular compact rheometer) available at IIT Ropar (Fig. 6) to obtain the shear stress values at various shear rates (0 - 1000 Sec^{-1}) and magnetic field intensity of 72 kA/m for all the prepared samples. The rheometer has been set at a temperature of 27 °C, and the gap is maintained at a level of 0.75 mm. The shear rate versus shear stress flow curves of all prepared MR samples at magnetic field intensity (H) = 72 kA/m are presented in Fig. 7. The fluid begins to flow only after attaining a certain shear stress value, stated as fluid yield stress. It reflects the fluid-structural strength that relies on MR fluid constituents and experienced field density. This experimentally obtained data is then fitted to some appropriate fluid model to find out the developed MR fluid yield stress.

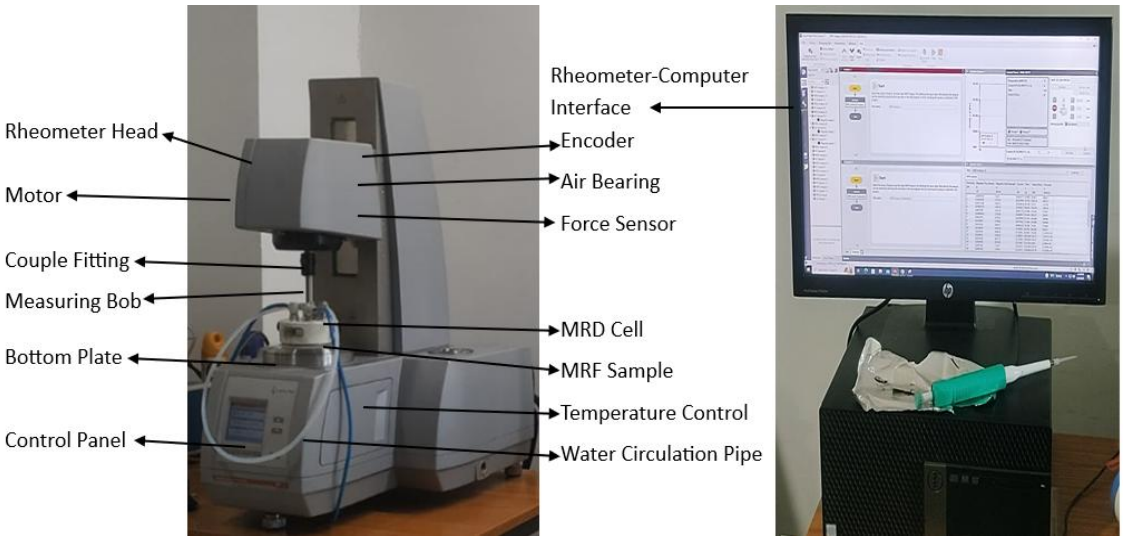

a b

Fig. 6 Modular compact rheometer (MCR-102): a – rheometer, b – computer attached to the rheometer

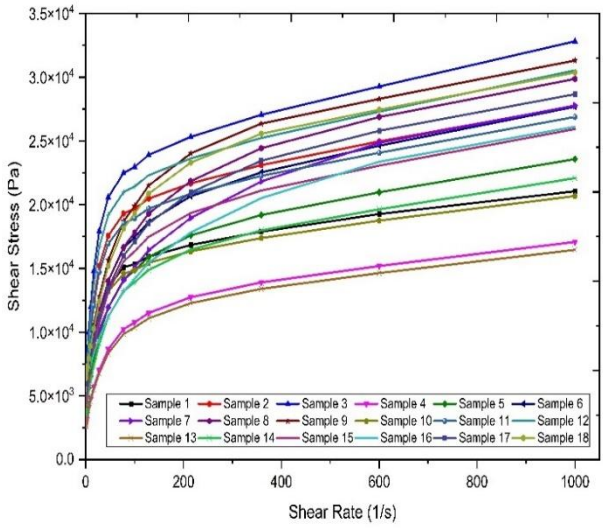

Fig. 7 Experimental flow curves of tested samples at 72 kA/m magnetic field intensity

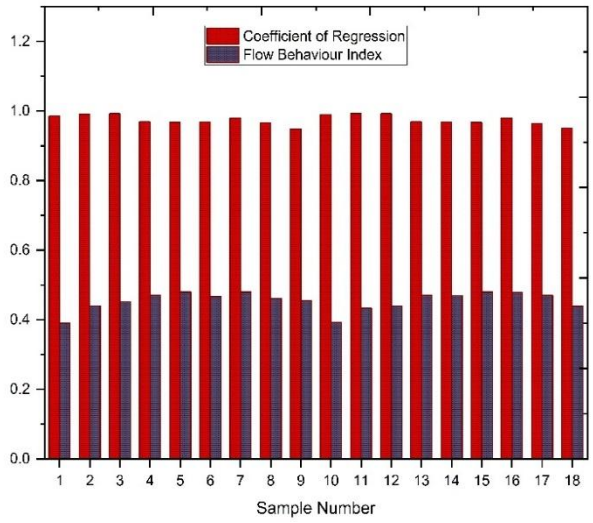

Fig. 8 Coefficient of regression and flow behavior index for all the samples as per the HB model

4. Determination of On-State Yield Stress (OYS)

The OYS of an MR fluid may be generally determined using Bingham Plastic, the Casson fluid model, and the Herschel-Bulkley flow model [37]. In the present study, the Herschel-Bulkley (HB) model has been utilized to estimate the yield stress values for prepared samples. The data attained from the rotational-oscillatory shear-type rheometer for all the samples is fitted in Eq. (1) of the Herschel-Bulkley model, where τ_o represents yield stress, τ denotes shear stress, n denotes fluid flow behavior index, K denotes consistency coefficient, and $\dot{\gamma}$ denotes shear rate

$$\tau = \tau_o + K\dot{\gamma}^n . \quad (1)$$

The regression coefficient (R^2) for all the prepared samples has been estimated to attain the goodness of fit for the experimentally obtained data relative to the used model. The R^2 values along with the flow behavior index (n) are shown in Fig. 8, where R^2 values signify that the experimentally obtained data have been well-fitted with the used fluid

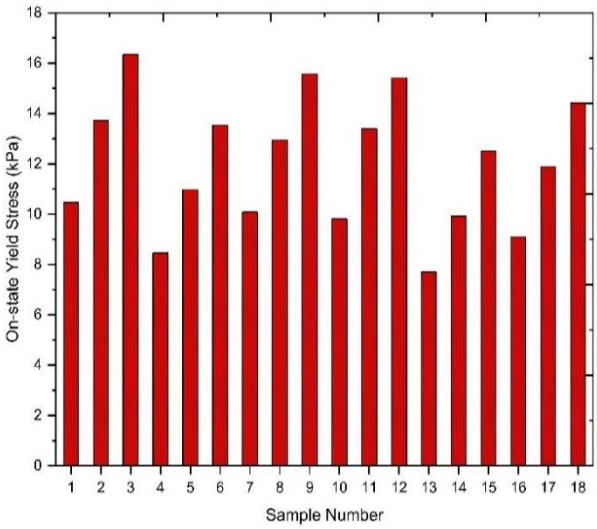

Fig. 9 On-state yield Stress (OYS) for all 18 prepared MR samples

model. The estimated value of the flow behavior index for all the prepared samples is less than unity, which represents the presence of the shear-thinning phenomenon.

The values of OYS at 72 kA/m along with their signal-noise (S/N) ratios for every sample have been shown in Table 3, and OYS values are also qualitatively shown in Fig. 9.

Table 3
On-state Yield Stress (OYS) for prepared MR samples

Sample No.	On-state Yield Stress, kPa	S/N ratio, dB
1	10.46	20.39
2	13.72	22.74
3	16.34	24.26
4	8.46	18.54
5	10.97	20.80
6	13.54	22.63
7	10.08	20.06
8	12.94	22.23
9	15.57	23.84
10	9.81	19.83
11	13.39	22.53
12	15.41	23.75
13	7.70	17.73
14	9.92	19.93
15	12.50	21.94
16	9.09	19.17
17	11.88	21.49
18	14.42	23.18

5. Analysis of Experimental Data

The Minitab 17.0 software has been used to analyze the response parameter, i.e., OYS, and to acquire crucial information about the design.

5.1. Determination of *S/N* ratio

Taguchi's technique proposed the idea of the S/N ratio, Eq. (2), to compute the deviation in the quality characteristics from their desirable value. The estimated S/N ratio in case of OYS using the larger-is-better criteria is expressed as follows:

$$S/N\ Ratio = -10 log \sum \frac{1}{y_i^2}, \quad (2)$$

where n represents several experiments, and y_i stands for the OYS associated with the i^{th} experiment. The *S/N* ratios in the case of OYS for all prepared MR samples are presented in Table 3.

The responses obtained for the S/N ratio along with means in case of the OYS for prepared MR fluid are presented in Fig. 10 and Fig. 11. The optimal value for response yield stress has been determined by identifying the greatest

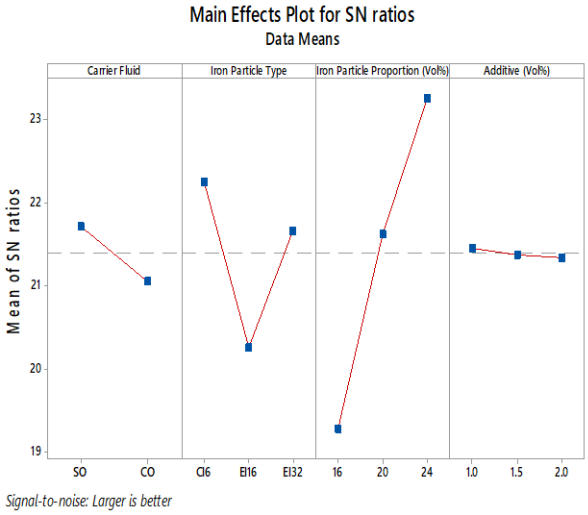

Fig. 10 Plots for the main effects of S/N ratios

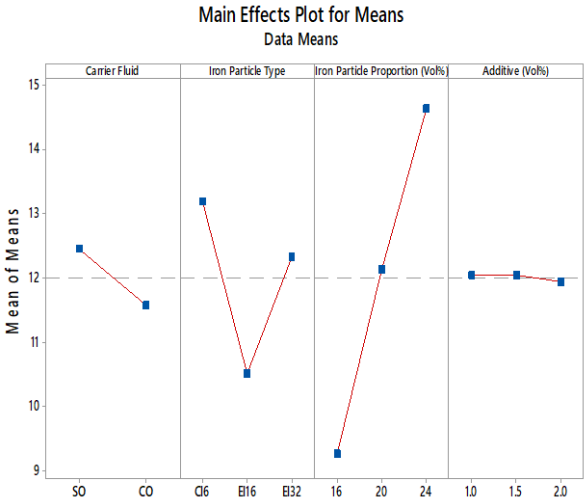

Fig. 11 Plots for the main effects of mean

value of the parameters among their levels. The optimal set of various selected input parameters (shown in Table 4) for OYS is obtained as $A_1B_1C_3D_1$.

The optimal set of input parameters ($A_1B_1C_3D_1$) is not available in the design table of the OA L_{18} (Table 2); hence, a confirmational test is recommended for validating the predicted results.

Table 4
Selected parameter levels for predicting the optimal value for on-state yield stress (OYS)

Para-meters	Carrier Fluid 'A'	Iron Particle Type 'B'	Iron Particle Proportion (vol%) 'C'	EGMS (vol%) 'D'
Parameter Level	1	1	3	1
Parameter Value	Silicon Oil	CI6	24%	1.0%

Fig. 10 and Fig. 11 exhibit that the fluid OYS largely depends upon the iron particle proportion (vol.%), iron particle type, and the used carrier fluid. It may also be determined that iron (Fe) particle proportion (vol.%) exhibits the largest departure from the center line and hence may be entitled as the most significant parameter. Iron particle

type and carrier fluid also show a notable departure from the center line and are hence entitled as the second and third most important parameters for the MR fluid. The EGMS (vol%) parameter does not depart much from the central line, indicating its very little contribution towards the response parameter.

5.2. ANOVA results estimated for On-state Yield Stress (OYS)

The analysis of variance (ANOVA) is adopted to identify the significance of different input factors and their contribution (% age) to the selected response factor, i.e., the OYS. The results obtained at a 95% confidence level for OYS are presented in Tables 5, 6, and 7. The tables indicate that iron (Fe) particle proportion (vol%) is the highest significant factor (F-value = 511.47), followed by iron particle type (F-value = 132.28) and carrier fluid (F-value = 41.66). The obtained value for R^2 is reasonable as it is very close to 1. These results concluded that the iron particle proportion by vol% is the most predominant factor that affects the OYS, contributing 76.36%, followed by the iron particle type, contributing 19.75%, the carrier fluid, having a contribution of 3.11%, and EGMS by vol % has a contribution of less than 0.1%.

Table 5

Response table for S/N ratios for On-state Yield Stress (OYS)

Level	Carrier Fluid	Iron Particle Type	Iron Particle Proportion (vol%)	EGMS (vol%)
1	21.73	22.25	19.29	21.46
2	21.06	20.26	21.63	21.38
3	-----	21.67	23.27	21.35
Delta	0.66	1.99	3.98	0.11
Rank	3	2	1	4

Table 6

Response table for the mean of Means for On-state Yield Stress (OYS)

Level	Carrier Fluid	Iron Particle Type	Iron Particle Proportion (vol%)	EGMS (vol%)
1	12.453	13.188	9.267	12.043
2	11.569	10.515	12.137	12.040
3	-----	12.330	14.630	11.940
Delta	0.884	2.673	5.363	0.110
Rank	3	2	1	4

Table 7

Analysis of Variance for On-state Yield Stress (OYS)

Source	DF	Seq SS	Adj MS	F-Value	P-Value	%-age Contribution	Remarks
Carrier Fluid	1	3.520	3.520	41.66	<0.001	3.11%	Significant
Iron Particle Type	2	22.355	11.177	132.28	<0.001	19.75%	Significant
Iron Particle Proportion (vol% %)	2	86.438	43.219	511.47	<0.001	76.36%	Significant
EGMS (vol%)	2	0.046	0.0228	0.27	0.769	0.04%	---
Error	10	0.845	0.0845	---	---	0.75%	---
Total	17	113.204	---	---	---	100.00%	---
R - sq. = 99.25%, R - sq. (adj) = 98.73%							
DF: Degree of freedom, Adj MS: Adjusted mean squares, Seq SS: Sequential sum of squares							

5.3. Computation of on-state yield stress using confidence interval about estimated mean

The optimal input parameters combination to maximize the MR fluid's OYS are given as carrier fluid at the first level, i.e., silicon oil; iron particle type at the first level, i.e., CI6; iron particle proportion (vol%) at the third level, i.e., 24%; and EGMS (vol%) at the first level, i.e., 1%. The optimum yield stress (kPa) has been estimated for the optimal set of input parameters, i.e., $A_1B_1C_3D_1$. The predicted value for the mean value of the OYS is obtained [38, 39] as:

$$\bar{\mu}_{OYS} = \bar{A}_1 + \bar{B}_1 + \bar{C}_3 + \bar{D}_1 - 3\bar{T}\,, \tag{3}$$

where $\bar{T}$: overall mean of OYS = 12.01, $\bar{A}_1$: average OYS at the first level of carrier fluid = 12.45, $\bar{B}_1$: average OYS at the first level of iron particle type = 13.18, $\bar{C}_3$: average OYS

at the third level of iron particle proportion (vol%) = 14.63, $\bar{D}_1$: average OYS at the first level of EGMS (vol%) = 12.04. Putting these determined values in Eq. (3), the estimated mean of OYS has been obtained.

$$\bar{\mu}_{OYS} = 12.45 + 13.18 + 14.63 + 12.04 - 3 \times 12.01 = \\ = 16.28, \text{ kPa}. \quad (4)$$

The 95 percent confidence interval for confirmational experiments (CI_{CE}) and population (CI_{POP}) is obtained by utilizing Eqs. (5) and (6) [39]:

$$CI_{CE} = \sqrt{F_{\alpha}(1, f_e) V_e \left[\frac{1}{\eta_{eff}} + \frac{1}{R}\right]}, \quad (5)$$

$$CI_{POP} = \sqrt{\frac{F_{\alpha}((1, f_e) V_e}{\eta_{eff}}}, \quad (6)$$

where α represents the risk, $F_{\alpha}(1, f_e)$ denotes the F-ratio for the confidence level of $(1-\alpha)$ against DF, i.e., 17, and f_e represents error DF = 10, N represents the number of results, i.e., 18 (treatment is taken as 18 and repetition as 1), R represents the size of the sample for confirmational experiments and is taken as 1, V_e represents the error variance, i.e., 0.0845. The effective sample size (η_{eff}) is used for treatment conditions and predicted as follows:

$$\eta_{eff} = \frac{N}{1 + Total\ DF} = \frac{18}{1+7} = 2.25. \quad (7)$$

The tabulated F value $\{F_{0.05}(1,10)\}$ is taken as 4.96 [39] for the confidence level of 95%, i.e., $(1-\alpha)$. Putting these values in Eqs. (5) and (6) provide the values for CI_{CE} and CI_{POP}. These are as follows:

$$CI_{CE} = \sqrt{4.96 \times 0.0845 \left[\frac{1}{2.25} + \frac{1}{1}\right]} = \pm 0.778, \quad (8)$$

$$CI_{POP} == \sqrt{\frac{4.96 \times 0.0845}{2.25}} = \pm 0.432. \quad (9)$$

The optimal range of the predicted OYS (kPa) based on CI_{CE} is given as:

$$\mu_{OYS} - CI_{CE} < \mu_{OYS} < \mu_{OYS} + CI_{CE}, \quad (10)$$

$$15.502 < \mu_{OYS} < 17.058. \quad (11)$$

The 95% confidence interval for the estimated mean of the OYS (kPa) in the case of CI_{POP} is given as:

$$\mu_{OYS} - CI_{POP} < \mu_{OYS} < \mu_{OYS} + CI_{POP}, \quad (12)$$

$$15.848 < \mu_{OYS} < 16.712. \quad (13)$$

The value of OYS has been computed using Eq. (4), i.e., 16.28 kPa, which lies within the 95 percent confidence interval for the estimated mean of OYS for CI_{CE} as well as CI_{POP}.

5.4. Experimental validation of results for the optimal MR fluid

To obtain the OYS experimental value by employing an optimal input parameter combination suggested by ANOVA, the MR fluid sample is synthesized and experimentally examined. A value of 16.56 kPa for OYS has been computed for the optimal predicted sample. This obtained OYS value lies within the 95 percent confidence interval for the estimated mean of OYS for the CI_{CE} and CI_{POP} as computed using Eqs. (11), and (13). The experimentally obtained value (16.56 kPa) for the optimal MR fluid sample agrees well with the value computed using Eq. (4) (16.28 kPa), and just a marginal percentage error has been observed.

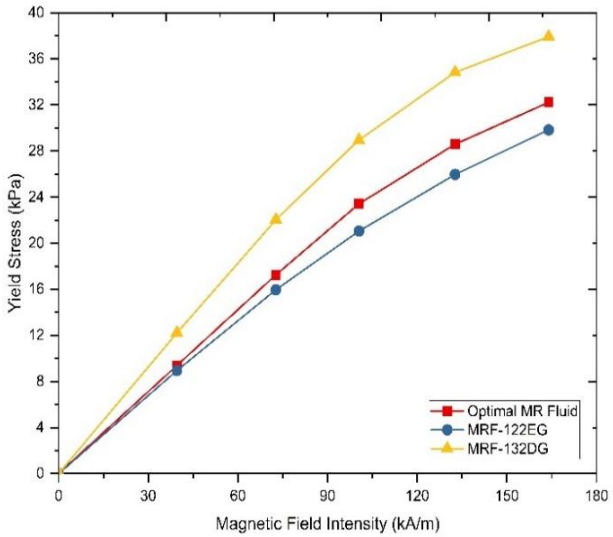

Fig. 12 Comparison of optimal MR fluid with Lord MRF-122EG and Lord MRF-132DG fluid

5.5. Comparison of optimal MR fluid with Lord MRF-122EG and Lord MRF-132DG fluid

To correlate the outcomes of the prepared optimal MR fluid, commercially available fluids Lord MRF-132DG and Lord MRF-122EG, manufactured by Lord Corporation, USA [40], are chosen, and their OYS values are correlated.

Fig. 12 exhibits that the OYS for the optimal in-house prepared MR fluid is higher in comparison to the Lord MRF-122EG fluid but lower in comparison with the Lord MRF-132DG fluid at all values of applied magnetic fields. Thus, the optimal MR fluid, having a significant value of OYS, has been prepared and may be adequately utilized in developing various MR devices.

6. Results and Discussion

The influence of various components of the synthesized MR fluid on the OYS has been expressed as follows.

6.1. Influence of magnetic particles proportion

The proportion of magnetic particles suspended in the MR fluids has a significant impact on its OYS. The OYS is enhanced by increasing the proportion of iron (Fe) particles, as shown in Fig. 10 and Fig. 11. It occurs due to improved magnetic saturation because of a larger proportion of magnetic particles suspended in a definite amount of the carrier fluid. The occupancy of a larger amount of magnetic particles leads to a denser structure for the identical value of the applied field. Due to this, higher stress is needed to break the highly dense MR fluid's structure.

6.2. Influence of magnetic particle type

The OYS for the MR fluid having the carbonyl iron of 6-micron size (CI6) is higher (Fig. 10 and Fig. 11) as compared to the other 2 types of iron particles used for this study. This depicts that carbonyl iron particles generate higher OYS in comparison with the electrolytic iron particles. The EI particles of 16-micron size (EI16) show a higher value of the OYS as compared to EI particles of 32-micron size (EI32), indicating that large-sized particles produce higher OYS in comparison with the smaller-sized particles.

6.3. Influence of magnetic flux intensity

The flow curve (OYS vis-a-vis magnetic field) for the optimal MR fluid sample has been presented in Fig. 12. The magnetic field is a major contributing parameter that enhances the MR fluid stiffness. The magnetic interactions between Fe particles are enhanced with an increased magnetic field, which induces a stronger bonding of the particles. However, it is restricted to a certain value which depends on the particle's saturation magnetization.

7. Conclusions

In the present study, the impact of various constituents of the in-house synthesized MR fluid on its On-state Yield Stress (OYS) has been investigated. All the synthesized MR fluid samples are characterized based on their OYS values. In conformity with the obtained results, the following conclusions are depicted:

- Among the 18 prepared MR fluid samples, Sample No 03 exhibits the maximum value of the OYS, and Sample no. 13 exhibits the lowest value for it.
- From the optimization study, the optimal parametric combination is summed up to be $A_1B_1C_3D_1$ i.e., "first level of parameter A (carrier fluid), the first level of parameter B (iron particle type), third level of parameter C (iron particle proportion by vol%) and the first level of parameter D (EGMS by vol%)".
- By computing the mean of the OYS at all the levels of input variables, iron particle proportion by vol% has been ranked first in deciding the selected response, followed by iron particle type, carrier fluid, and EGMS by vol%.
- Analysis of variance results concluded that the iron particle proportion by vol% is the most prominent factor that impacts the OYS with a contribution of 76.36%, followed by the iron particle type with a contribution of 19.75%, carrier fluid with a contribution of 3.11% and EGMS (vol%) has a contribution of less than 0.1%.
- The obtained value (16.56 kPa) of OYS for the optimal predicted sample lies within the 95 percent confidence interval for the estimated mean of OYS for the CI_{CE} and CI_{POP}.
- The comparison results exhibit that the OYS for the optimal in-house prepared MR fluid follows the same pattern as followed by Lord MRF-122EG and Lord MRF-132DG at all values of applied magnetic fields.

Conflict of Interest

The authors declare no conflict of interest.

References

1. **Jolly, M. R.; Bender, J. W.; Carlson, J. D.** 1999. Properties and Applications of Commercial Magnetorheological Fluids, Journal of Intelligent Material Systems and Structures 10(1): 5-13. https://doi.org/10.1177/1045389X9901000102.
2. **Premalatha, S. E.; Chokkalingam, R.; Mahendran, M.** 2012. Magneto Mechanical Properties of Iron Based MR Fluids, American Journal of Polymer Science 2(4): 50-55. https://doi.org/10.5923/j.ajps.20120204.01.
3. **Mangal, S. K.; Kumar, A.;** 2015. Experimental Studies of In-House Developed Magnetorheological Fluid in a Damper, International Journal of Performability Engineering 11(3): 257-264.
4. **Kamble, V. G.; Kolekar, S.; Madivalar, C.** 2015. Preparation of Magnetorheological Fluids Using Different Carriers and Detailed Study on Their Properties, Current Research in Nanotechnology 6(1): 7-15. https://doi.org/10.3844/ajnsp.2015.7.15.
5. **Sarkar, C.; Hirani, H.** 2015. Synthesis and Characterization of Nano-Copper-Powder Based Magnetorheological Fluids for Brake, International Journal of Scientific Engineering and Technology 4(2): 76-82.
6. **Liu, J.; Wang X.; Tang, X.; Hong, R.; Wang, Y.; Feng W.** 2015. Preparation and characterization of carbonyl iron/strontium hexaferrite magnetorheological fluids, Particuology 22: 134-144. https://doi.org/10.1016/j.partic.2014.04.021.
7. **Jain, D.; Avchare, K. R.** 2016. Design, Fabrication and Testing of Low Cost Magneto- Rheological Fluid Brake Testing Machine, Research and Reviews: Journal of Material Sciences 4(2): 20-25. https://doi.org/10.4172/2321-6212.1000141.
8. **Vėžys, J.; Dragašius, E.; Volkovas, V.; Mystkowski, A.; Korobko, E.** 2016. The sedimentation of magnetorheological fluid monitoring system based on resistivity measuring, Mechanika 22(5): 449-452. https://doi.org/10.5755/j01.mech.22.5.14958.
9. **Arief, I.; Sahoo, R.; Mukhopadhyay, P. K.** 2016. Effect of temperature on steady shear magnetorheology of CoNi microcluster-based MR fluids, Journal of Magnetism and Magnetic Materials 412: 194-200. https://doi.org/10.1016/j.jmmm.2016.04.004.

10. **Guo, Y. Q.; Xu, Z. D.; Chen, B. B.; Ran, C. S.; Guo W. Y.** 2017. Preparation and Experimental Study of Magnetorheological Fluids for Vibration Control, International Journal of Acoustics and Vibration 22(2): 194-201. https://doi.org/10.20855/ijav.2017.22.2464.
11. **Laherisheth, Z.; Upadhyay, R. V.** 2017. Influence of particle shape on the magnetic and steady shear magnetorheological properties of nanoparticle based MR fluids, Smart Materials and Structures 26(5): 054008. https://doi.org/10.1088/1361-665X/aa54a1.
12. **Gurubasavaraju, T. M.; Kumar, H.; Arun, M.** 2017. Evaluation of optimal parameters of MR fluids for damper application using particle swarm and response surface optimisation, Journal of the Brazilian Society of Mechanical Sciences and Engineering 39: 3683-3694. https://doi.org/10.1007/s40430-017-0875-9.
13. **K. P. L.; Kumar, D.; Hirani, H.** 2017. Synthesis and field dependent shear stress evaluation of stable MR fluid for brake application, Industrial Lubrication and Tribology 69(5): 655-665. https://doi.org/10.1108/ILT-03-2016-0061.
14. **Nagdeve, L.; Sidpara, A.; Jain, V. K.; Ramkumar, J.** 2018. On the effect of relative size of magnetic particles and abrasive particles in MR fluid-based finishing process, Machining Science and Technology 22(3): 493-506. https://doi.org/10.1080/10910344.2017.1365899.
15. **Guo, Y. Q.; Sun, C. L.; Xu, Z. D.; Jing, X.** 2018. Preparation and Tests of MR Fluids With CI Particles Coated With MWNTs, Frontiers in Materials 5: 50. https://doi.org/10.3389/fmats.2018.00050.
16. **Dorosti, A. H.; Ghatee, M.; Norouzi, M.** 2020. Preparation and characterization of water-based magnetorheological fluid using wormlike surfactant micelles, Journal of Magnetism and Magnetic Materials 498: 166193. https://doi.org/10.1016/j.jmmm.2019.166193.
17. **Vėžys, J.; Dragašius, E.; Juzėnas, K.; Korobko, E.; Mystkowski, A.** 2019. Comparison of different magneto-rheological fluids' stability, Journal of Measurements in Engineering 7(2): 84-89. https://doi.org/10.21595/jme.2019.20200.
18. **Marins J.A.; Plachý T.; Kuzhir P.** 2019. Iron–sepiolite magnetorheological fluids with improved performances, Journal of Rheology 63(1): 125-139. https://doi.org/10.1122/1.5048051.
19. **Zhu, W.; Dong, X.; Huang, H.; Qi, M.** 2019. Iron nanoparticles-based magnetorheological fluids: A balance between MR effect and sedimentation stability, Journal of Magnetism and Magnetic Materials 491: 165556. https://doi.org/10.1016/j.jmmm.2019.165556.
20. **Aruna, M. N.; Rahman, M. R.; Joladarashi, S.; Kumar, H.** 2019. Influence of additives on the synthesis of carbonyl iron suspension on rheological and sedimentation properties of magnetorheological (MR) fluids, Materials Research Express 6(8): 086105. https://doi.org/10.1088/2053-1591/ab1e03.
21. **Jinaga, R.; Jagadeesha, T.; Kolekar, S.; Choi, S.B.** 2019. The Synthesis of Organic Oils Blended Magnetorheological Fluids with the Field-Dependent Material Characterization, International Journal of Molecular Sciences 20(22): 5766. https://doi.org/10.3390/ijms20225766.
22. **Zhang, Y.; Li, D.; Cui, H.; Yang, J.** 2020. A new modified model for the rheological properties of magnetorheological fluids based on different magnetic field, Journal of Magnetism and Magnetic Materials 500: 166377. https://doi.org/10.1016/j.jmmm.2019.166377.
23. **Seo, Y.; Choi, H. J.** 2020. Core–shell-structured Fe_3O_4 nanocomposite particles for high-performance/stable magnetorheological fluids: preparation and characteristics, Journal of the Korean Ceramic Society 57: 608-631. https://doi.org/10.1007/s43207-020-00070-9.
24. **Huang, H.; Chen, C.; Zhang, Z. C.; Zheng, J. N.; Li, Y. Z.; Chen, S. M.** 2020. Design and experiment of a new structure of MR damper for improving and self-monitoring the sedimentation stability of MR fluid, Smart Materials and Structures 29(7): 075019. https://doi.org/10.1088/1361-665X/ab8839.
25. **Srivastava, M.; Pandey, P. M.; Kuldeep; Basheed, G. A.; Pant, R. P.** 2021. Synthesis and characterization of the rheological behavior of MR fluid for polishing silicon wafer using double-disc chemical-assisted magnetorheological finishing process, Journal of Magnetism and Magnetic Materials 534: 168044. https://doi.org/10.1016/j.jmmm.2021.168044.
26. **Xu, Z. D.; Sun, C. L.** 2021. Single-double chains micromechanical model and experimental verification of MR fluids with MWCNTs/GO composites coated ferromagnetic particles, Journal of Intelligent Material Systems and Structures 32(14): 1523-1536. https://doi.org/10.1177/1045389X20988779.
27. **Maurya, C. S.; Sarkar C.** 2021. Synthesis and characterization of novel flake-shaped carbonyl iron and water-based magnetorheological fluids using laponite and oleic acid with enhanced sedimentation stability, Journal of Intelligent Material Systems and Structures 32(14): 1624-1639. https://doi.org/10.1177/1045389X20987001.
28. **Han, S.; Choi, J.; Han, H. N.; Kim, S.; Seo, Y.** 2021. Effect of Particle Shape Anisotropy on the Performance and Stability of Magnetorheological Fluids, ACS Applied Electronic Materials 3(6): 2526-2533. https://doi.org/10.1021/acsaelm.1c00070.
29. **Gedik, E.; Kurt, H.; Pala, M.; Alakour, A.** 2022. An experimental and artificial neural network investigation on the laminar flow of magnetorheological fluids through circular pipes, Journal of Magnetism and Magnetic Materials 546: 168893. https://doi.org/10.1016/j.jmmm.2021.168893.
30. **Choi, S. B.** 2022. Sedimentation Stability of Magnetorheological Fluids: The State of the Art and Challenging Issues, Micromachines 13(11): 1904. https://doi.org/10.3390/mi13111904.
31. **Tong, Y.; Zhao, P.; Li, X.; Ma, N.; Dong, X.; Niu, C.; Wu, Z.; Qi, M.** 2022. Properties and mechanism of ionic liquid/silicone oil based magnetorheological fluids, International Journal of Smart and Nano Materials 13(2): 263-272. https://doi.org/10.1080/19475411.2022.2069876.
32. **Kumar, S.; Sehgal, R.; Wani, M.F.; Sharma, M. D.; Ziyamukhamedova, U.; Dar, T. A.** 2023. Next-generation ecofriendly MR fluid: Hybrid GO/Fe2O3

encapsulated carbonyl iron microparticles with improved magnetorheological, tribological, and corrosion resistance properties, Carbon 214: 118331. https://doi.org/10.1016/j.carbon.2023.118331.

33. **Zhao, P.; Du, T.; Ma, N.; Dong, X.; Qi, M.** 2023. Effect of interfacial shear strength between magnetic particles and carrier liquid on rheological properties of magnetorheological fluids, Journal of Molecular Liquids 369: 120929. https://doi.org/10.1016/j.molliq.2022.120929.
34. **Maharani, E. T.; Lee, D. H.; Kim, Y. J.; Oh, J. S.; Choi, S. B.** 2024. The Actuating Characteristics of Magnetorheological Fluids Subjected to Particle Sedimentation and Temperature Variation, Actuators 13(8): 277. https://doi.org/10.3390/act13080277.
35. **Horak, W.; Stępień, B.; Sapiński, B.** 2024. Experimental study of magnetorheological fluids under large periodic deformations, Smart Materials and Structures 34(1): 015027. https://doi.org/10.1088/1361-665X/ad9442.
36. **Wiener, T.; Offenzeller, C.; Berger, D.; Jakoby, B.** 2024. In situ monitoring of the iron content in magnethorheological rotary actuators, Smart Materials and Structures 33(11): 115044. https://doi.org/10.1088/1361-665X/ad85b4.
37. **Chauhan, V.; Kumar, A.; Sham, R.** 2024. Magnetorheological fluids: A comprehensive review, Manufacturing Review 11: 6. https://doi.org/10.1051/mfreview/2024005.
38. **Ross, P. J.** 1988. Taguchi techniques for quality engineering. New York: McGraw-Hills Book Company. 279p.
39. **Roy, R. K.** 1990. A primer on the Taguchi method, New York: Van Nostrand Reinhold. 247p.
40. MRF-122EG Magneto-Rheological Fluid. Available at: https://www.shoplordmr.com/mr-products/mrf-122eg-magneto-rheological-fluid-250ml.

V. Chauhan, A. Kumar, R. Sham

SYNTHESIS AND RHEOLOGICAL CHARACTERIZATION OF MAGNETORHEOLOGICAL FLUIDS

S u m m a r y

Magnetorheological (MR) fluids correspond to the kind of smart materials capable of varying their rheological characteristics, i.e., viscosity, yield stress, etc., on varying the magnetic field. In this article, 18 MR fluid samples utilizing various constituents are prepared and optimized with the aid of an L_{18} orthogonal array. The synthesized samples are experimentally tested on a rotational oscillatory shear rheometer, namely MCR-102 (modular compact rheometer), to obtain the shear stress values at various shear rates (0 - 1000 Sec^{-1}). This experimentally obtained data is fitted to the Herschel-Bulkley fluid model to estimate the On-state Yield Stress (OYS) for the tested MR fluid samples. An optimal set of the selected parameters, i.e., silicon oil (carrier fluid), CI6 as the type of iron particle, 24 (Vol%) of iron particle proportion, and EGMS (1.0% by volume), has been obtained using Taguchi analysis. An experimental verification test on the MR fluid with the Taguchi predicted optimal set of parameters has been performed, and OYS matches well with its statistically predicted value. The ANOVA results examine the contribution of input parameters and present that the iron particle proportion is the most prominent parameter that impacts the OYS, contributing 76.36%, followed by iron particle type which contributes 19.75%, carrier fluid with a contribution of 3.11% and additive proportion has a contribution of less than 0.1%. The OYS values for the optimal MR fluid are compared with commercially available MR fluids, i.e., Lord MRF-122EG and Lord MRF-132DG, at various magnetic field intensities (0 - 164 kA/m). The comparison results exhibit that the OYS for the optimal in-house prepared MR fluid follows the same pattern as followed by Lord MRF-122EG and Lord MRF-132DG at all values of applied magnetic fields.

Keywords: MR fluid, viscosity, on-state yield stress, analysis of variance, Herschel Bulkley model.

Received May 7, 2024
Accepted June 25, 2025